Frascati Physics Series Vol. XVI (2000), pp. 000-000
PHYSICS AND DETECTORS FOR DAΦNE – Frascati, Nov. 16-19, 1999

The DEAR Target and Detector System

presented by
Johann Zmeskal

on behalf of the DEAR collaboration
M. Augsburger[j], G. Beer[b], S. Bianco[c], A. M. Bragadireanu[c,i], M. Bregant[d], W. H. Breunlich[a], M. Cargnelli[a], D. Chatellard[j], J. -P. Egger[k], F. L. Fabbri[c], B. Gartner[a], C. Guaraldo[c], R. S. Hayano[f], M. Iliescu[c,**], T. Ishiwatari[e], T. M. Ito[c,l], M. Iwasaki[e], R. King[a], P. Knowles[j], T. Koike[h], B. Lauss[c,⋆], V. Lucherini[c], J. Marton[a], E. Milotti[d], F. Mulhauser[j], S. N. Nakamura[g], C. Petrascu[c,**], T. Ponta[i], A. C. Sanderson[b], L. A. Schaller[j], L. Schellenberg[j], H. Schneuwly[j], R. Seki[l,m], D. Tomono[e], T. Yoneyama[e], E. Zavattini[d], J. Zmeskal[a]

[a]Institute for Medium Energy Physics, Austrian Academy of Sciences, Boltzmanng. 3, A-1090 Vienna, Austria
⋆on leave of absence from above
[b]Univ. of Victoria, Dept. of Physics and Astronomy, P.O. Box 3055, Victoria, Canada
[c]INFN - Laboratori Nazionali di Frascati, Via E. Fermi 40, I-00044 Frascati , Italy
[d]Univ. degli Studi di Trieste, Dip. di Fisica and INFN Sezione di Trieste, Via A. Valerio 2, I-34127, Trieste, Italy
[e]Tokyo Institute of Technology, 2-12-1 Ookayama Meguro, Tokyo 152, Japan
[f]Univ. of Tokyo, Dept. of Physics, 7-3-1 Hongo, Bunkyo, Tokyo 113, Japan
[g]Inst. of Physical and Chemical Research (RIKEN), 2-1 Hirosawa, Wako, Saitama 351-01, Japan

[h]KEK, High Energy Accelerator Research Organization, Tanashi Campus
3-2-1 Midori, Tanashi, Tokyo 188, Japan
[i]Inst. of Physics and Nuclear Engineering "Horia Hulubei", Dept. of High Energy Physics, P.O. Box MG-6 R-76900 Magurele, Bucharest, Romania
**on leave of absence from above
[j]Univ. de Fribourg, Inst. de Physique, Bd. de Perolles, CH-1700 Fribourg, Switzerland
[k]Univ. de Neuchâtel, Inst. de Physique, 1 rue A.-L. Breguet, CH-2000 Neuchâtel, Switzerland
[l]W.K. Kellogg Radiation Laboratory, Calif. Inst. of Technology, Pasadena, CA 91125, USA
[m]Dep. of Physics and Astrophysics, California State Univ., Northridge, CA 91330, USA

ABSTRACT

The DEAR experimental setup, consisting of the cryogenic target system and the CCD-detectors, is described. The results obtained in systematic measurements of the background in the DEAR interaction region are presented.

1 Introduction

The objective of DEAR is the determination of the isospin-dependent $\overline{K}N$ scattering lengths via the measurement of the strong interaction shifts and widths of the kaonic hydrogen and deuterium K-series lines [1)].

The scientific aim of DEAR is an understanding of SU(3) chiral symmetry breaking, through the determination of the KN sigma terms. The KN sigma terms are also a sensitive and direct measurement of the strangeness content of the nucleon [2)].

The main challenge to DEAR is to detect a very weak x-ray signal out of the background of an e^+e^- collider with high statistics and high precision.

The scientific program of DEAR will be developed in two stages: with an NTP (NTP = Normal Temperature Pressure) target and with a cryogenic target (hydrogen and deuterium).

2 The DEAR experimental setup

The principle of the DEAR experiment is straightforward: low momentum negative kaons, produced by decay of the ϕ-meson, leave the thin-wall beam pipe, are degraded in energy to a few MeV, enter a gaseous hydrogen (deuterium)

target through a thin window and are finally stopped in the hydrogen gas. The stopped kaons are captured in an outer orbit of the hydrogen atoms forming an exotic kaonic hydrogen atom. The kaons cascade down and some of them will reach low-n states from which they feel strong interaction and can reach the ground state by emitting X rays. The energy of the X rays emitted in these transitions (K-series lines) is measured with a CCD (Charge-Coupled Device) detector system [3].

2.1 The Cryogenic Target

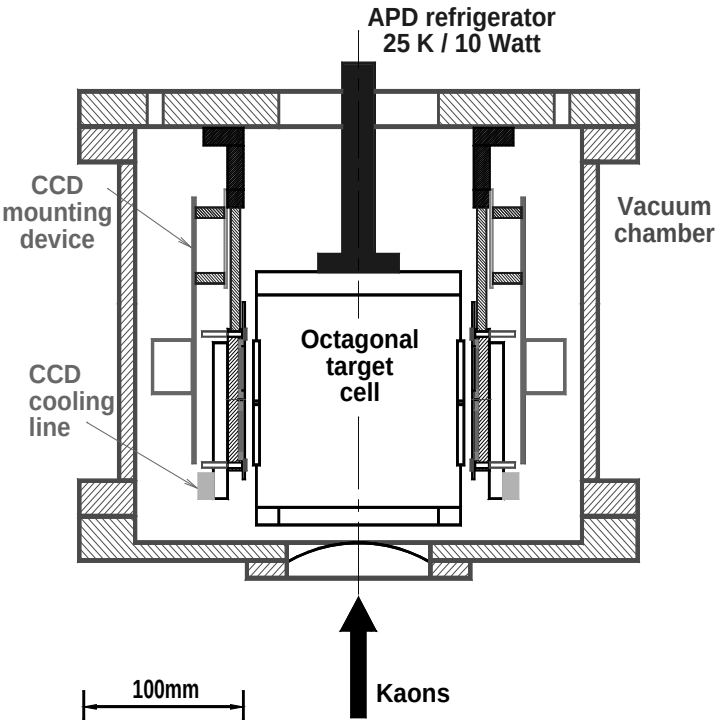

Figure 1: The sideview of the cryogenic hydrogen gas target cell (25 K / 3 bar) surrounded by the CCD detector system.

The octagonal target cell shown in figure 1 is made of specially selected aluminum alloy for the cell body (AlMgSi0.5). For the window frames pure alu-

minum Al (99.98 %) was used to avoid interference from x-ray lines coming from components such as Fe or Mn present in most common aluminum alloys. The cell has a side length of 55 mm and a height of 140 mm. On each of the eight side-walls are two thin Kapton windows (50 μm) facing the CCD surfaces. The absorption in the window material is less than 5 % for 5 keV X rays. The kaon entrance window has a diameter of 100 mm and is also made of Kapton with a thickness of 190 μm. The distance from the entrance window to the center of the beam pipe is approximately 110 mm.

The target cell, surrounded by the CCD mounting devices, is placed in the center of the vacuum chamber, connected via a copper cylinder to the two-stage closed-cycle helium refrigerator (APD-Croygenics DE-204SLB). The refrigerator system provides a cooling power of about 10 watts at 25 K. The insulation vacuum is maintained to better than 10^{-5} mbar using a wide-range turbomolecular pump (Varian 300HT). The hydrogen gas target cell (ultra-pure hydrogen gas purified by a Pd diffusion device will be used) will typically operate with a temperature of 25 K, stabilized to better than 0.2 K. With a gas pressure of 3 bar, a gas density of 3.6 mg/cm^3 (approx. 5 % of liquid hydrogen density) will be achieved, corresponding to a gas pressure at room temperature of about 50 bar. Each of the CCD mounting devices will hold two CCD-22 chips, for a total detection area of 11.5 cm^2 per holder. Two groups of four CCD mounting devices are connected via a flexible copper band to a closed-cycle refrigerator (APD CryoTiger) to keep the CCD in a temperature range between 150 and 170 K (in order to reduce thermal noise).

2.2 The CCD Detector

The essential CCD concept is to store information in the form of electrical charge in potential wells within a semiconductor. These potential wells are created by the influence of overlying electrodes separated from the semiconductor by a thin insulating layer. The potential wells, and therefore the charge packets, are shifted through the semiconductor by applying phased voltages to the electrodes, providing a means of extracting the stored information. Present-day CCDs are typically silicon-based MOS (metal-oxide semiconductor) devices with a square pixel structure with a typical side length of tens of microns. In standard devices, three electrodes are required for each row of pixels, which are divided into columns by channel stops in the semiconductor. When a CCD is in accumulation mode, a negative voltage is applied to two electrodes and a positive voltage to the third, creating independent potential wells in each pixel. During the readout, alternating potentials are applied to these three electrodes, shifting the accumulated electrons to a special readout line at the end of the columns.

CCDs are ideal for a wide range of applications in the energy range from a few eV up to about 20 keV. Even though CCDs cannot be triggered, their background rejection capabilities are very powerful, a necessity for the extraction of a weak signal from a large background, which is one of the characteristics of

kaonic hydrogen experiments. In fact, in the very low-energy region, typical of exotic-atom research, CCDs can have a better signal-to-background ratio than triggered Si(Li) detectors.

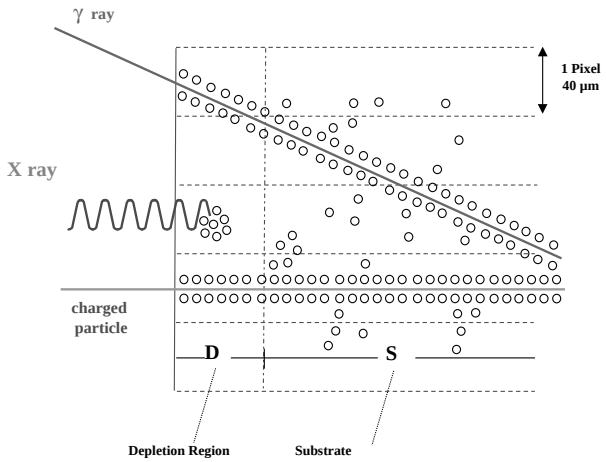

Figure 2: Sketch of the interaction of charged particles, γ rays and X rays in the detection area of the CCD detector. While X rays have a high probability to interact within the depletion region of a single pixel (mainly via the photoelectric effect) this is only true for a negligible part of γ rays and charged particles, which produce charges also in the substrate of the chip where they can diffuse and create multi-pixel events.

This characteristic is based on the fact that X rays (up to about 10 keV) normally deposit all of their energy in a single pixel, whereas the energy from charged particles, gammas and neutrons, which constitute the background, is normally distributed over several pixels. In silicon, these X rays interact almost exclusively by the photoelectric effect, and the deposited energy is normally localized in space within the depletion layer (30-40 μm for the deep depleted CCDs used in DEAR), whereas charged particles loose energy by ionization everywhere in the bulk material ($\sim$500 μm thick). This behaviour is sketched in figure 2. The electrons from the electron-hole pairs created in the depletion layer cannot escape from the induced potential wells, but the electrons created in the bulk material can move freely, causing charge to be collected in multiple adjacent pixel cells. Since every pixel has eight adjacent pixels, the usual way to distinguish X rays from background events is to examine the eight neighboring pixels and confirm that the charge they contain is consistent with the noise level. If this is true, the event is considered an X ray. Therefore, a good X ray

event is defined as a single pixel with energy above the noise level surrounded by 8 pixels with signals statistically consistent with noise. Using this single pixel criterion it is possible to eliminate almost all background events except for soft X rays. The huge background reduction which is possible with CCDs is shown in figure 3.

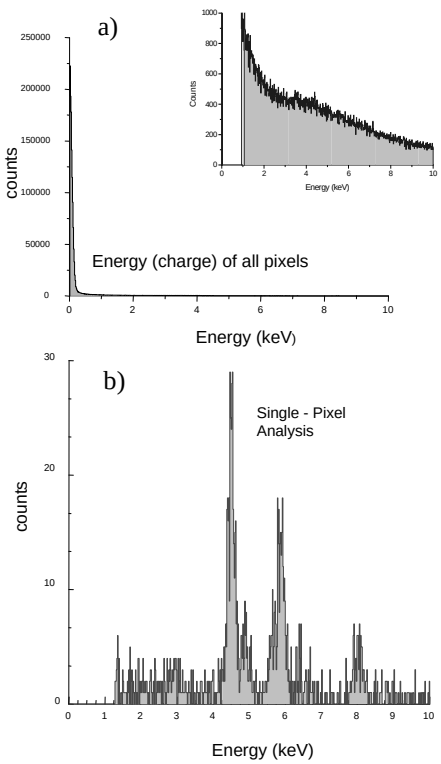

Figure 3: Demonstration of the enormous background rejection capability of a CCD detector. a) shows the energy spectrum which is observed when all pixels of a CCD chip are plotted. The dominance of the noise peak at the energy zero point is obvious. The magnified region shows the region interesting for the experiment. b) The same energy spectrum after application of the single-pixel analysis. X ray lines from fluorescence excitation of Ti, Mn and Cu are visible.

The accumulation period (exposure time) for the CCDs should not be so long as to permit the same 9-pixel cluster to be hit multiple times ("blindness"). If this occurs, valid x-ray events will be lost through the single pixel cut. Blindness is caused by excessive background events. To avoid this, the number of pixel-hits should not exceed a few percent, which corresponds to a

maximum of approximately 5000 background events per CCD.

The readout electronics for the CCD system, shown in figure 4, consists of four major components: readout boxes, command box, VME crate, and data acquisition computer. The readout boxes contain phase generators for transferring signal charges out of the CCD during a readout, as well as amplifiers to shape and amplify the analog signal. To minimize the noise introduced by the analog sampling of the CCDs, a correlated double-sampling technique is used in which the output of the CCD is sampled with and without the signal, and the results are subtracted to eliminate the contrast reset level of the amplifiers. This technique lengthens the readout time, but minimizes the noise such that the remaining dominant noise is the output amplifier noise. With this technique, the transfer and readout time is 64 μs per pixel, with a total readout time of about 28 s per CCD, which is shorter than the typical exposure times, and is not a problem since data accumulation continues throughout the readout.

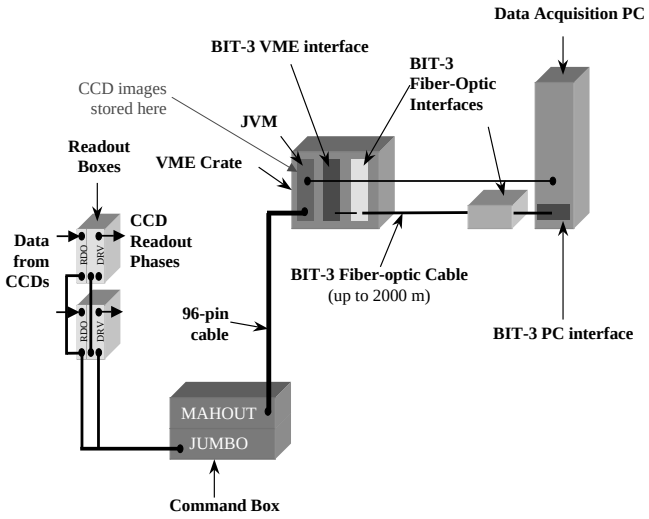

Figure 4: Sketch of the electronic modules used for the readout of the CCD detectors. The analog signal from the chip is amplified in the readout boxes, where the chip driving signals are also created, then digitized in the command box and sent via an opto-coupled VME link to the data storage on a PC located in the control room.

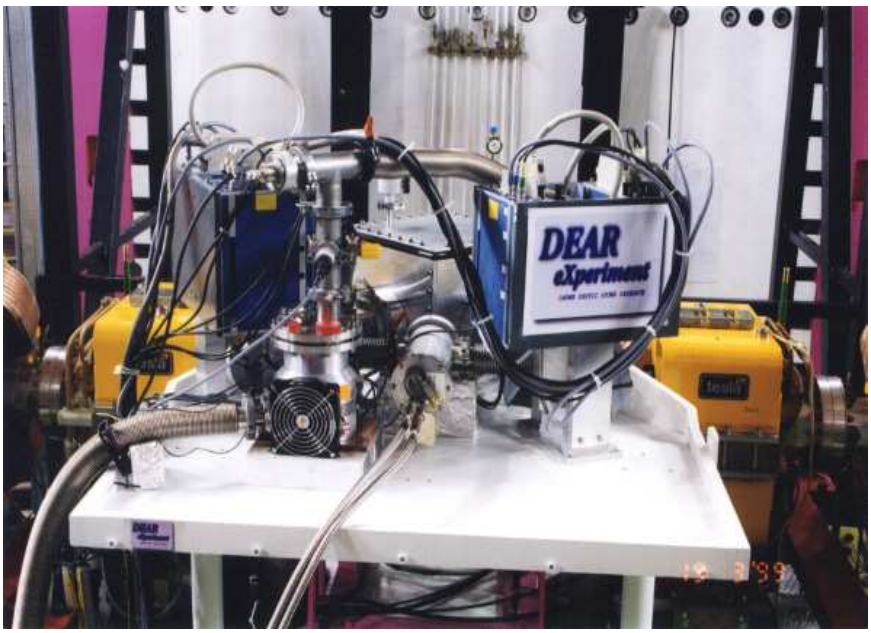

Figure 5: The installed NTP setup in the DAΦNE hall as seen from inside the rings.

3 The NTP setup

The purpose of the NTP setup (a photo of the setup presently installed in the DAΦNE hall is shown in figure 5) is to measure background, compare it to the Monte Carlo calculation, and tune the degrader thickness by optimizing the signal from the kaonic nitrogen $7 \rightarrow 6$ transition at $\sim$4.5 keV. The yield of this signal is higher (about ten times) than that of the kaonic hydrogen K_α line, so faster feedback is possible. The target cell is a cubic box made of pure aluminum (30 cm $\times$ 30 cm $\times$ 35 cm), 1.5 cm thick, which is placed above the specially designed DEAR beam pipe in the DEAR interaction region. Two CCD housings made of aluminum, each one containing two CCD chips are mounted on circular openings of the two chamber walls which are on the inner side of the DAΦNE main rings. The CCDs operate in a vacuum of 10^{-5} mbar (maintained with a turbomolecular pump) and at a temperature of $\sim$160 K. An APD Cryotiger refrigerator is used to cool the CCDs to the working temperature. Two 50 μm thick Kapton windows separate the CCDs' vacuum from the target chamber, which is filled with nitrogen at atmospheric pressure. The target chamber and the CCD detectors were shielded with copper and lead for most of the performed measurements.

3.1 Background measurements at DAΦNE

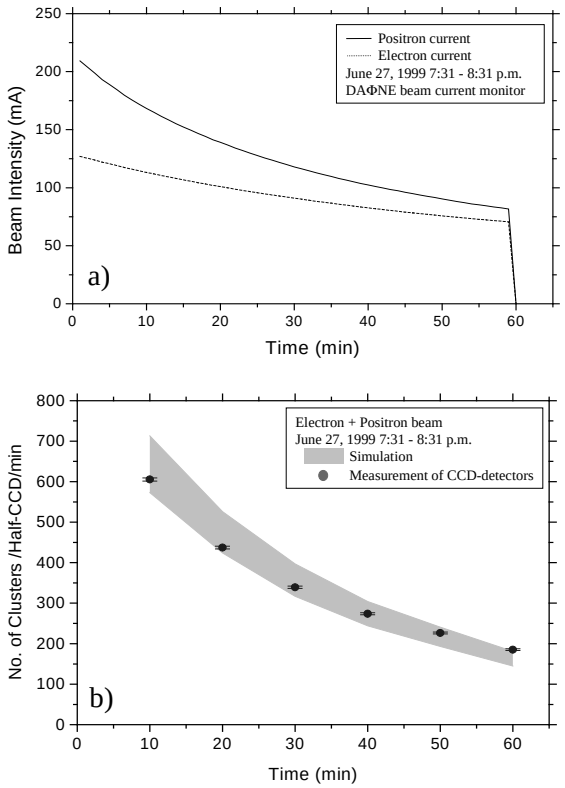

Figure 6: a) Beam intensities for simultaneously circulating electron and positron beams, separated in the DEAR interaction region, as given by the DAΦNE beam monitor. b) Observed number of clusters per half-CCD per minute (filled circles) during the corresponding beam period. The shaded area shows the results of the DEAR Monte Carlo simulation.

Two different types of background events affect the CCD detector. The first type is ionizing particles hitting the CCDs, which appear as cluster events. These background events can be rejected by the single-pixel analysis method but, with an increasing number of hits, the x-ray detection efficiency decreases - the CCDs become "blind". Because the CCDs are time-integrating detectors, one must select the exposure time to guarantee only small occupancies. An evaluation of the overall background is also used to determine the level of

"blindness" of the CCDs and therefore the exposure time. Consequently, the amount of shielding required to allow acceptable working conditions can be deduced as well.

The second type of background is X rays, which cannot be rejected and therefore must be taken into account. They contribute to the accidental background in the x-ray energy spectrum and originate in the particles lost from the beam, which can give rise to e.m. showers.

3.2 Background from circulating beams

Using the NTP setup, the following type of beams have been monitored by observing the number of clusters created in the CCD chips in the period from March to July 1999 [4]: only electron beams, only positron beams, and electron and positron beams circulating at the same time but kept separated in the DEAR interaction point. It should be made clear that, in the considered beam periods, no collisions between e^- and e^+ were produced in the DEAR interaction region and, consequently, the additional background coming from beam-beam dynamics could not be studied. Figure 6 shows an example of the performed measurement with non-colliding electron and positron beams. The time behavior of the number of clusters follows the time behavior of the number of injected electrons and positrons, as given by the DAΦNE beam monitor. The measurements of the background from circulating beams were compared with Monte Carlo simulations, taking into account beam intensity, beam lifetime and vacuum conditions [4]. The results of the DEAR Monte Carlo simulation are in very good agreement with the measured data, as can be seen in the example given in figure 6.

3.3 X-ray background from circulating beams

The study of the x-ray background is especially important because the final statistical precision of the DEAR experiment will critically depend on the level of the x-ray background. The observed x-ray energy spectrum, shown in figure 7, is the result of about two weeks of measurements with circulating, but not colliding, electron and positron beams with the shielded setup. The detection range of the CCDs was set from 0.8 keV up to 16.5 keV for this measurement. At low energy the fluorescence lines of aluminum, the material of the target and detector housing and silicon, the material of the CCD chips, are clearly seen. In addition, on the high energy side, the electronic K_α peak of a zirconium foil was measured. This foil was placed inside the NTP target for online energy scale calibration. No line structure can be seen in the region of interest (from 5.55 keV to 6.75 keV). In particular one observes no structure at the energies of the electronic x-ray transitions coming from manganese and iron, materials normally existing in aluminum alloys. This demonstrates, quite clearly, the high purity of the selected aluminum for each component.

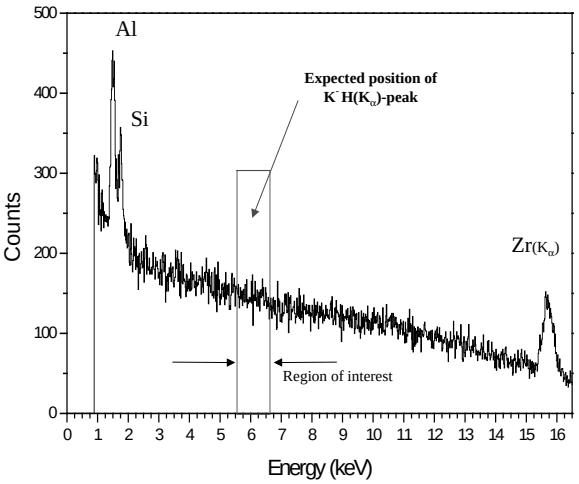

Figure 7: X-ray energy spectrum observed in ∼2 weeks with circulating beams. A zirconium foil was inserted into the target to provide an online energy calibration peak. The corresponding electronic x-ray peak together with the one originating in the aluminum of the detector and target housing and the silicon material of the CCD chip can clearly be observed. No line structure is visible in the region of interest where the kaonic hydrogen K_α peak is expected.

4 Conclusions

Extensive studies have been performed to constrain the possible systematic errors of the measurement coming from energy calibration, detector stability and linearity, as well as analysis and fitting procedures.

The fact that the Monte Carlo simulation could reproduce, also quantitatively, the observed features of the interaction region with circulating beams, gives us confidence in our assessment of the expected background, which principally determines the statistical precision of the experiment.

The presented results suggest that the DEAR configuration can indeed reach the planned challenging level of precision.

References

1. S. Bianco *et al.*, LNF-98/039 (P) (1998); Rivista del Nuovo Cimento, **22**, no.11, 1 (1999).
2. C. Guaraldo, These proceedings.
3. J.-P. Egger, D. Chatellard and E. Jeannet, Part. World **3**, 139 (1993).
4. M. Augsburger *et al.*, LNF-99/32(P) (1999), submitted to Nucl. Instr. and Methods A.